NRC·CNRC

NRC Publications Archive
Archives des publications du CNRC

Numerical Simulation of Broken Ice Cover Forces on Structures: a Parametric Study

Barker, A.; Sayed, M.; Timco, G. W.

This publication could be one of several versions: author's original, accepted manuscript or the publisher's version. / La version de cette publication peut être l'une des suivantes : la version prépublication de l'auteur, la version acceptée du manuscrit ou la version de l'éditeur.

Publisher's version / Version de l'éditeur:

Proceedings 2000 Annual Conference of the Canadian Society for Civil Engineering, Proceedings CSCE'00, G, pp. 243-249, 2000

NRC Publications Record / Notice d'Archives des publications de CNRC:
https://nrc-publications.canada.ca/eng/view/object/?id=fe4c2e32-b480-442b-933a-5e9b1d584bc5
https://publications-cnrc.canada.ca/fra/voir/objet/?id=fe4c2e32-b480-442b-933a-5e9b1d584bc5

Access and use of this website and the material on it are subject to the Terms and Conditions set forth at
https://nrc-publications.canada.ca/eng/copyright
READ THESE TERMS AND CONDITIONS CAREFULLY BEFORE USING THIS WEBSITE.

L'accès à ce site Web et l'utilisation de son contenu sont assujettis aux conditions présentées dans le site
https://publications-cnrc.canada.ca/fra/droits
LISEZ CES CONDITIONS ATTENTIVEMENT AVANT D'UTILISER CE SITE WEB.

Questions? Contact the NRC Publications Archive team at PublicationsArchive-ArchivesPublications@nrc-cnrc.gc.ca. If you wish to email the authors directly, please see the first page of the publication for their contact information.

Vous avez des questions? Nous pouvons vous aider. Pour communiquer directement avec un auteur, consultez la première page de la revue dans laquelle son article a été publié afin de trouver ses coordonnées. Si vous n'arrivez pas à les repérer, communiquez avec nous à PublicationsArchive-ArchivesPublications@nrc-cnrc.gc.ca.

National Research Council Canada | Conseil national de recherches Canada

Canada

Proceedings 2000 Annual Conference of the Canadian Society for Civil Engineering
Proceedings CSCE'00, Vol. G, pp 243-249, London, Ont. Canada, 2000.

NUMERICAL SIMULATION OF FLOATING ICE FORCES ON BRIDGE PIERS

A. Barker, M. Sayed, and G. W. Timco
Canadian Hydraulics Centre, National Research Council, Ottawa, Canada

ABSTRACT:

A numerical model of river ice interaction with bridge piers is presented. The model is based on a Particle-In-Cell (PIC) approach combined with a viscous plastic ice rheology. The plastic yield follows a Mohr-Coulomb criterion. The Zhang-Hibler (1997) numerical scheme is used to solve the momentum equations. The model is used in this paper to examine the role of the shape of the structure, ice thickness, ice properties, and velocity on the resulting ice forces. The results show good agreement with field measurements.

1. INTRODUCTION

Estimates of ice forces on bridge piers involve uncertainties, which motivated several field measurements and numerical studies. There have been numerous programs of measurements. Recently, Johnston et al. (1999) presented an overview and analysis of available data, including the measurements at Hondo, Pembridge, Rideau and St. Regis Rivers piers. Numerical simulations of river ice interaction with hydraulic structures include a discrete element formulation by Daly and Hopkins (1998). Lu and Shen (1998) used both a viscous plastic and an elastic viscous plastic continuum rheology to model river ice transport.

The present work uses a model developed earlier for ice forecasting (Sayed and Carrieres, 1999). It was also used by Sayed et al. (2000) to study pack ice forces on wide offshore structures. The present implementation of the model employs a continuum rheology based on a cohesive Mohr-Coulomb yield criterion. The viscous plastic approach of Hibler (1979) is used to numerically approximate the rigid-plastic idealization. Furthermore, a Particle-In-Cell (PIC) approach (Flato, 1993) is used to account for ice advection. The solution of the governing equations follows the implicit scheme of Zhang and Hibler (1997), that provides significant computational efficiency. The numerical formulation of the various aspects of the model has been covered by Sayed and Carrieres (1999), and in the above references. The emphasis of this work is rather on examining the appropriate choice of material properties, predicting forces on bridge piers, and verification of the numerical results.

In the following sections of the paper, a brief description of the numerical model is given. The analysis of ice-pier interaction follows. Next, the resulting forces and behaviour of the ice cover are presented. The results are then compared to field measurements and other calculation methods. Finally, conclusions are presented.

2. MODEL

2.1 Governing Equations

The ice cover is represented by a two-dimensional formulation. Thickness, however, is allowed to change. An assembly of discrete particles represents the ice according to the PIC approach. Each particle has a volume, which remains constant. The area of each particle may be reduced, and the thickness accordingly increases, as pressure increases. This situation would correspond to increasing ice thickness. Thus, ice pile-up and ridging can be accounted for. Note that ice growth and decay are not a concern for the present problem.

The linear momentum and rheology equations govern the movement and deformation of the ice cover. Particles are individually advected in a Lagrangian manner. Therefore, a continuity equation is not needed. The linear momentum equations include the inertial terms, water drag, and gradient of the internal ice stress, and are expressed as follows

$$[2.1] \quad \rho_{ice} h \frac{d\vec{u}}{dt} = \nabla \cdot \sigma + \vec{\tau}_w$$

where ρ_{ice} is the ice density, h is the ice thickness, $\vec{u}$ is the velocity vector, σ is the stress tensor, and $\vec{\tau}_w$ is the water drag stress. Water drag stress is given by the following quadratic formula

$$[2.2] \quad \vec{\tau}_w = c_w \rho_w \left| \vec{\mathbf{U}}_w - \vec{u} \right| \left(\vec{\mathbf{U}}_w - \vec{u} \right)$$

where c_w is the water drag coefficient, $\vec{U}_w$ is water velocity, and ρ_w is water density.

Rheology is introduced by the following general stress-strain rate relationship,

$$[2.3] \quad \sigma_{ij} = -p\delta_{ij} + 2\eta \dot{\varepsilon}_{ij} + (\zeta - \eta)\dot{\varepsilon}_{kk}\,\delta_{ij}$$

where $\dot{\varepsilon}_{ij}$ is the strain rate, p is the mean normal stress, η is the shear viscosity, and ζ is the bulk viscosity. The common assumption of zero bulk viscosity is used here.

The mean normal stress, p, is expected to increase with increasing ice compactness, A (area of ice/total area). Hibler (1979) presented the following formula

$$[2.4] \quad p = P^* h_{ice} \exp\left(-K(1-A)\right)$$

where P^* is a reference ice strength, and K is a constant. Other variations of Eq. (2.4) may be used (see for example Lu and Shen, 1998).

In order to satisfy the Mohr-Coulomb criterion, the shear viscosity, η, is assigned the following value

$$[2.5] \quad \eta = \frac{\left(c\cot\phi + p\right)\sin\phi}{\Delta}$$

where ϕ is the angle of internal friction, and c is the cohesion. The strain rate Δ is given by

$$[2.6] \quad \Delta = \max\left(\left| \dot{\varepsilon}_1 - \dot{\varepsilon}_2 \right|, \dot{\varepsilon}_0 \right)$$

where $\dot{\varepsilon}_1$ and $\dot{\varepsilon}_2$ are the principal strain rates and $\dot{\varepsilon}_0$ is a threshold strain rate. At small rates of deformation, the shear viscosity becomes constant, and the corresponding rheology would be viscous. Otherwise the deformation is plastic. A very small threshold strain rate (typically $\dot{\varepsilon}_0 = 10^{-20}\ s^{-1}$) is used in order to maintain a predominantly plastic deformation.

2.2 Numerical Approach

The numerical approach is briefly outlined in this section. A comprehensive treatment of the subject is outside the scope of this paper, and would be too lengthy to include here. Details of the present numerical formulation, however, were covered in Sayed and Carrieres (1999).

The momentum and rheology equations are solved using an Eulerian (fixed) grid. The semi-implicit finite difference method of Zhang and Hibler (1997) is used.

The method is based on uncoupling the velocity components and employing an over-relaxation scheme. An iteration loop is also carried out to ensure that the yield condition is satisfied.

For the PIC formulation, a bilinear interpolation function is used. At each time step the velocities are interpolated from the grid to each particle. Thus, particles can be individually advected. From the new positions, values of particle area and mass are mapped to the grid. The resulting ice mass and area for each grid cell are then used to update ice thickness and concentration. The present discussion is intended to briefly convey the essential aspects of the PIC formulation. See Sayed et al. (2000) for more details.

The solution steps can be summarized as follows. Particles are advected to their new positions. The area and mass of each particle are next mapped to the grid. The ice area and mass for each grid cell are in turn used to determine ice thickness and concentration on the grid. At that point, the momentum and rheology equations are solved on the grid. Finally the resulting velocities are mapped from the grid to the particles. The preceding operations are repeated for each time step.

2.3 Boundary conditions

Solution of the momentum equations incorporates specified velocity values at boundary nodes. Zero velocities, for example, can be specified at fixed boundaries to give a *no slip* condition. Constant (non zero) velocity values can also be specified at boundary nodes, which is useful in modelling oncoming ice that may be considered to enter a study area under constant velocity. A velocity mask is used in the present model to identify boundary nodes and specify the velocities of those nodes.

The PIC formulation is convenient for dealing with free boundaries at the interface between ice-covered areas and open water. The particles can move at such an interface, and no conditions need to be prescribed. Open water nodes, however, should have the appropriate velocities. This is accomplished by solving the momentum equations over the open water nodes of the grid.

The use of particles also makes it possible to introduce a *full slip* boundary condition. Allowing the particles to move freely parallel to a boundary satisfies that condition. The particles are not allowed, however, to cross that boundary (displacement perpendicular to the boundary is reset to zero).

3. TEST CASES

Simulation runs focused on a common pier geometry, consisting of a rectangular shape with a circular front. Zabilansky (1996) reported on detailed measurements of ice forces on such a pier in the White River. His measurements, along with similar measurements made by Sodhi et al. (1983), are used to verify the numerical results. The details of these field measurements are present in section 5.

Figure 1 shows a schematic of the numerical grid and the pier. The pier instrumented by Zabilansky (1996) was 1.22 m wide. A 200 by 85 node grid represents the study area. Grid cell size is 0.3 m. The grid thus covers 60 m along the length of the river, and 25.5 m along the width. Full *slip* boundary conditions were used at the top and bottom of the grid, which represent riverbanks. If a particle moved, for example, through the top boundary, its y-position would be changed to bring it back within the grid without changing its x-position. A no slip boundary condition was used for the pier. Velocities of the nodes within the pier were set to zeros. Additionally if a particle crossed the boundary of the pier, its normal displacement was reset to zero. The latter procedure accounted for the circular shape of the pier. Note that just fixing node velocities to zeros would produce a step-like boundary for the pier instead of a circular one.

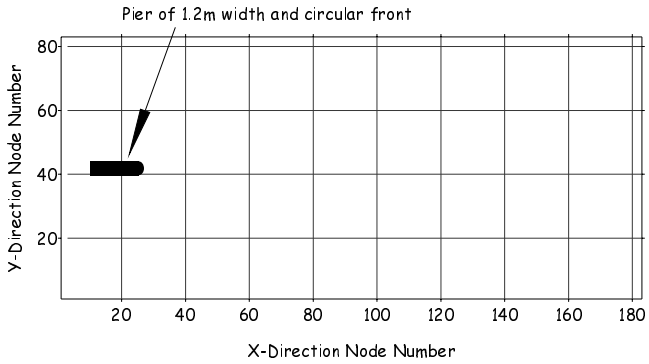


Figure 1 Base grid

The ice cover was driven against the pier by imposing a constant velocity upstream. The constant driving velocity was applied to a 36 m wide zone at the upstream side (node number 80 to 200 along the x-direction, Fig. 1). The relatively large size of that zone ensured that a sufficient supply of particles would flow against the structure during the runs. A 7 m wide part of the grid adjacent to the downstream boundary was initialized with no ice. This allowed the ice cover to

move freely past the pier, without interference from the downstream edge of the grid.

Simulations were chosen to cover a range of plausible ice properties and other parameter values. The role of ice properties was examined by varying cohesion, c, angle of internal friction, ϕ, and compressive strength parameter, P^*. Several values of ice velocities and initial ice concentration were also used. In addition, preliminary runs examined the effect of grid cell size, number of grid nodes, and size of the time step. Those preliminary tests ensured that the chosen grid and time step do not introduce spurious numerical effects.

As an example, the results of a base case are presented here. The parameters used for that case are:

- Angle of internal friction, $\phi = 45^0$.
- Cohesion, c = 50 kPa.
- Compressive stress parameter, P^* (Eq. 2.4) = 100 kPa.
- Ice velocity = 0.5 m/s.
- Drag coefficient = 0.005.
- Time step = 0.1 s.

The resulting force on the pier is plotted versus time in Fig. 2. The force was estimated by summing the stress (along the x-direction) and multiplying this by grid cell length for the grid cells immediately in front (upstream) of the pier. The lateral force on the pier was approximately zero. The force shown in Fig. 2 reaches a maximum after approximately 17 s. A number of runs were done for different durations and grid sizes and showed that the force remains at that maximum value.

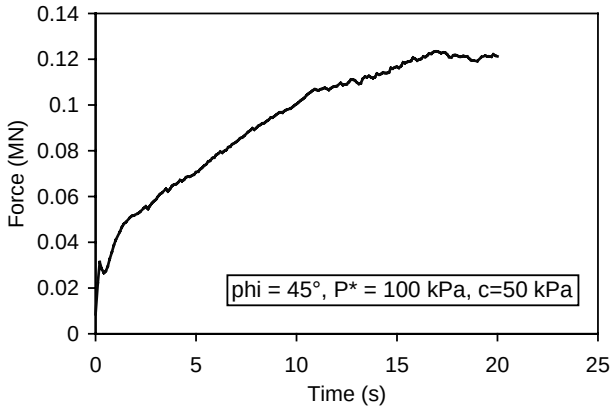


Figure 2 Force-time record for the base case

Contours of the normal stress in x-direction, and ice concentration are shown in Figs. 3 and 4, respectively. These plots, zoomed in to highlight the portion of the grid nearest the pier, show snapshots after approximately 15 s from the start of the run, which is slightly before the occurrence of the maximum force. The normal stress contours show higher values in a *bulb-shaped* zone in front of the pier, as would be expected. Concentration contours display a similar pattern, with high values in front of the pier. A concentration of one (full ice coverage) is evident in the high-pressure zone. There was no noticeable thickness build-up for the base run. That indicated that the compressive strength of the ice cover is relatively high. A weaker strength (lower P^*) would cause an increase of ice thickness in high-pressure zones (see for example Sayed et al. 2000).

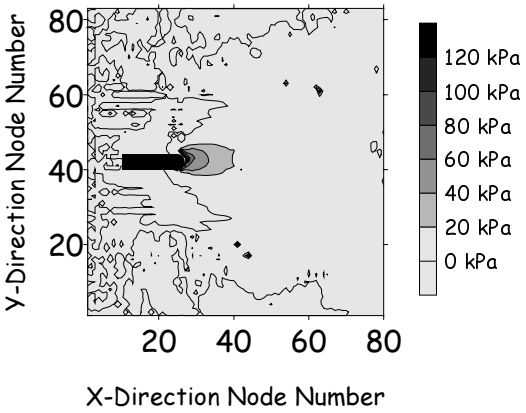


Figure 3 Normal stress in x-direction for base case run after 15 seconds

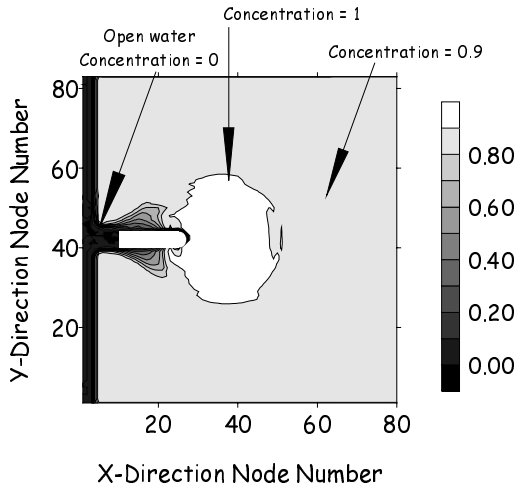


Figure 4 Concentration for base case after 15 seconds

Velocity vectors, which correspond to the above stress and concentration results, are plotted in Fig. 5. They show the expected behaviour of uniform values and direction away from the pier. The ice cover velocity, however, slows in front of the pier.

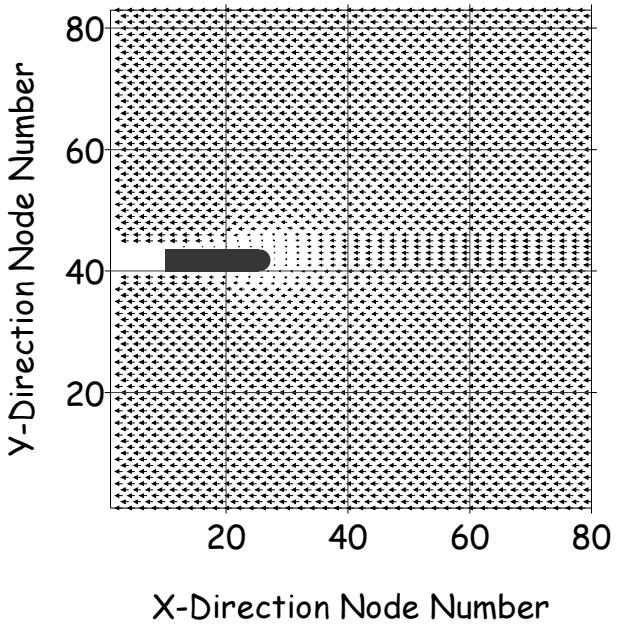


Figure 5 Velocity for base case after 15 seconds

4. PARAMETRIC STUDY

In addition to the base case, a parametric study was done, as mentioned earlier. The purpose was to determine sensitivity of the predicted forces to various factors and parameters, and to determine the appropriate parameter values that may lead to agreement with field measurements. The role of material properties is illustrated by plotting the force on the pier versus time for a range of values of the angle of internal friction, ϕ, in Fig. 6. A similar plot for different values of the cohesion, c, is shown in Fig. 7. All other variables remained similar to those of the base case.

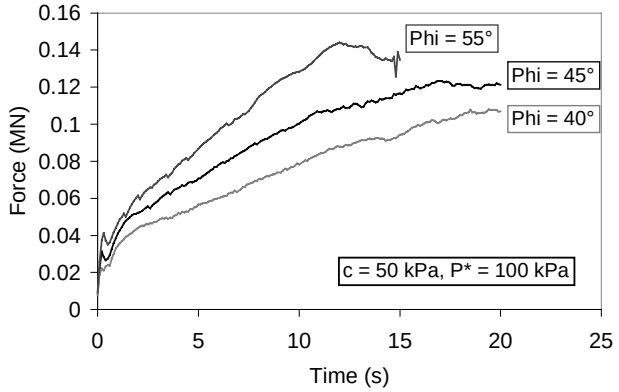


Figure 6 Force-time series for different values of ϕ

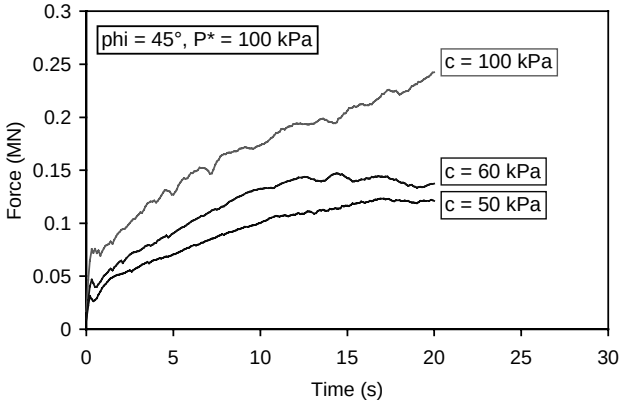


Figure 7 Force-time series for different values of cohesion

The results in Figs. 6 and 7 indicate that the cohesion has a significant influence on the predicted force. The peak force values range from 0.03 MN for zero cohesion to a value of 0.15 MN for a cohesion of 60 kPa. The angle of internal friction, ϕ has less influence on the force. The maximum force varied from 0.105 MN for $\phi = 40^{\circ}$, to 0.142 MN for $\phi = 55^{\circ}$.

Although there have been a number of studies investigating the behaviour of ice rubble, to the authors knowledge, there have not been any measurements made of the mechanical properties of loose, broken ice floes. Thus, in the present case, the model cannot use independently derived, mechanical properties. The range of values chosen for c and ϕ in these runs are in the range quoted for ice rubble (see e.g. Ettema and Urroz-Aguirre, 1991).

The role of ice velocity was examined by testing values ranging from 0.1 m/s to 0.5 m/s. The resulting forces are plotted versus time in Fig. 8. Somewhat surprisingly, ice velocity shows minor influence on the maximum force. This result may be explained by viewing the plot of velocity vectors in Fig. 5. It indicates that ice decelerates in a relatively small zone in front of the pier. Therefore the inertia effects would be small for the relatively narrow pier considered here. It should be noted, however, that this result should not be extrapolated to wide structures where the inertia of the ice cover may have more significant effects.

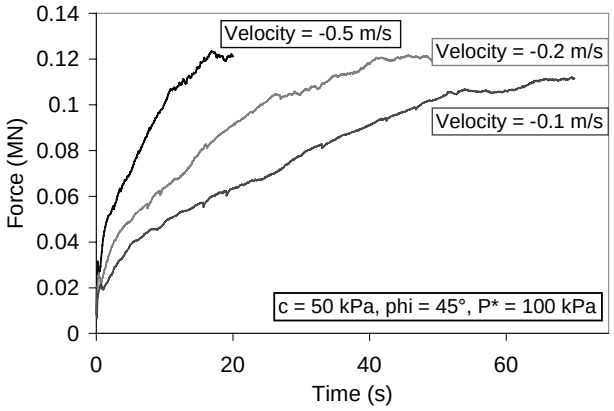


Figure 8 Force-time series for different ice velocities

5. COMPARISON WITH MEASUREMENTS AND OTHER CALCULATION METHODS

There have been several field investigations to measure the impact loads on a bridge pier with moving broken river ice. These measurements have recently been reviewed and summarized by Johnston et al. (1999). For the present case, there are 2 studies that are appropriate to cite. Sodhi et al (1983) reported on measurements of river ice interacting with a bridge pier on the Ottauquechee River in Vermont. In this case, the pier was vertical and 0.61 m wide with a V-shape. They reported a river ice run with floe sizes on the order of 1 to 10 m, with a thickness range of 0.15 m to 0.6 m. The maximum load was reported to be 0.12 MN, with a high static load of 0.11 MN. The static load occurred due to bridging of the ice floes between the pier and the shoreline. More recently, Zabilansky (1996) reported on measurements made on the White River in Vermont. In this case, the pier width was circular with a 1.22 m diameter with a 15° inclination. The river ice during the break-up run was about 0.25 to 0.45 m thick, with floe sizes ranging up to 5 m. The ice was in a single layer (i.e. no rafting) and of high concentration (0.75 to 0.95 coverage). Zabilansky reported maximum loads of 0.12 MN, with typical peak loads on the order of 0.04 to 0.06 MN.

The peak loads reported by Sodhi et al. (1983) and Zabilansky (1996) of 0.12 MN is in very good agreement with the loads predicted using the present model (see Figure 2 for a comparison with the base case). A good correlation between the present model and the reported peak measurements in full-scale tests was found using a cohesion of 50 kPa and a friction angle of 45°. It should be noted that the comparison in this case is directed towards the *peak* load measured during the field experiments. The time-series behaviour of the loading events is quite different for the two situations. In the numerical model, the load monotonically rises to a plateau value representing the peak value for the load. In the field measurements, the load variation is much more dynamic, as it represents numerous individual impact events. The numerical model essentially integrates the individual impacts to represent a continuum approach.

The conventional approach for predicting ice loads during dynamic loading events is to use a modified Korzhavin equation (Korzhavin 1971). The force (*F*) on the pier is given by

$$[5.1] \quad F = m\, I\, D\, h\, \sigma_o$$

where *m* is a shape factor (=0.9 for a circular pier), *I* is the indentation factor, *D* is the pier width, *h* is the ice thickness and σ_o is the nominal strength value. The original Korzhavin equation also includes a contact factor, but for impact loading, this coefficient is combined with the Indentation factor. Afanasev (1973) has given the combined Indentation coefficient as

$$[5.2] \quad I = (5\, h / D + 1)^{0.5}$$

for aspect ratios (D/h) less than 6. Sodhi et al. (1983) measured the compressive strength of the ice and report values in the range of 1.6 to 2.7 MPa. Assuming this strength range is appropriate for the White River ice, and using suitable values for pier width and maximum ice thickness, the calculated force on the White River pier is on the order of 1.5 to 2 MN. This load level is significantly higher than the measured peak value of 0.12 MN reported by Zabilansky (1996).

6. CONCLUSION

Ice forces on bridge piers were examined using a numerical model based on a PIC scheme for ice advection and a viscous plastic rheology. The model was modified from other versions used for ice forecasting and pack ice interaction with offshore structures. The main modification concerns the introduction of a cohesive Mohr Coulomb yield criterion. The simulations addressed a case of rectangular pier with circular front, and ice conditions that correspond to a well-documented program of field measurements. Those conditions were also chosen because they fall within the range commonly encountered.

The numerical simulations indicate that the model captures the main expected features of ice deformation. For example, the resulting distributions of stress, ice concentration and velocities follow the expected trends. The predicted force on the pier was also in agreement with available measurements.

A parametric study showed that cohesion of the ice cover has a significant effect on the predicted force. The angle of internal friction had a smaller effect. Tests with different ice velocity showed that velocity has a negligible effect on the force. Slenderness of the pier, which caused only a narrow zone of ice to decelerate, may explain this somewhat unexpected conclusion. It should not be extrapolated, however, for wide structures.

7. ACKNOWLEDGEMENTS

The financial support of the Program on Energy Research and Development (PERD) is gratefully acknowledged.

8. REFERENCES

Afanasev, V. 1973. Ice Pressure on Individual Marine Structures. *Ice Physics and Ice Engineering*, G. Yakovlev, Ed., Israel Program for Scientific Translation, pp 50-68.

Daly, S.F., and Hopkins, M.A. (1998). Simulation of river ice jam formation, *14th International Symposium on Ice*, ed. H-T. Shen, Potsdam, USA, Vol. 1, pp. 101-108.

Ettema, R. and Urroz-Aguirre, G. 1991. Friction and Cohesion in Ice Rubble Reviewed. *Cold Regions Engineering*, pp 316-325, ASME Specialty Conference, West Lebanon, NH, USA.

Flato, G.M. (1993). A Particle-In-Cell sea-ice model, *Atmosphere-Ocean*, Vol. 31, No. 3, pp. 339-358.

Hibler, W.D.III (1979). A dynamic thermodynamic sea ice model, *J. Physical Oceanography*, Vol. 9, No. 4, pp. 815-846.

Johnston, M., Timco, G. and R. Frederking. 1999. An Overview of Ice Load Measurements on Bridge Piers. *Workshop on River Ice*, J. Doering, Ed., pp 290-302, Winnipeg, Manitoba, Canada.

Korzhavin, K.N. (1971). *Action of ice on engineering structures*, US Army CRREL Translation TL260, Hanover, NH, USA.

Lu, S., and Shen, H-T. (1998). Constitutive laws for river ice dynamics, *14th International Symposium on Ice*, ed. H-T. Shen, Potsdam, USA, Vol. 1, pp. 109-116.

Sayed, M., and Carrieres, T. (1999). Overview of a new operational ice forecasting model, *ISOPE '99*, Brest, France, Vol. II, pp.622-627.

Sayed, M., Frederking, R.M.W., and Barker, A. (2000). Numerical simulation of pack ice forces on structures: a parametric study, to appear in Proceedings of the *10th International Offshore and Polar Engineering Conference (ISOPE '2000)*, Seattle, USA, May 28-June 2.

Sodhi, D., Kato, K. and Haynes, F.D. 1983. *Ice Force Measurements on a Bridge Pier in the Ottauquechee River, Vermont*. US Army CRREL Report 83-32, Hanover, NH, USA.

Zabilansky, L. 1996. *Ice Force and Scour Instrumentation for the White River, Vermont*. US Army CRREL Special Report 96-6, Hanover, NH, USA.

Zhang, J. and Hibler, W.D.III (1997). On an efficient numerical method for modelling sea ice dynamics, *J. Geophysical Research*, Vol. 102, No. C4, pp. 8691-8702